Electronic Supplementary Material (ESI) for ChemComm.
This journal is © The Royal Society of Chemistry 2019

Anionic Order and Band Gap Engineering in Vacancy Ordered Triple Perovskites

Taylor Hodgkins,† Christopher N. Savory,‡ Kelsey K. Bass,† Bethany Seckman,† David O. Scanlon,‡,¶ Peter I. Djurovich,† Mark E. Thompson,† and Brent C. Melot*,†

†*Department of Chemistry, University of Southern California, Los Angeles, CA 90089, USA*

‡*University College London, Kathleen Lonsdale Materials Chemistry, 20 Gordon Street, London WC1H 0AJ, United Kingdom*

¶*Diamond Light Source Ltd., Diamond House, Harwell Science and Innovation Campus, Didcot, Oxfordshire OX11 0DE, United Kingdom*

E-mail: melot@usc.edu

Methods

Experimental

Polycrystalline powders of $Cs_3Bi_2Br_{9-x}I_x$ were prepared by dissolving stoichiometric mixtures of CsI, CsBr, BiI_3, $BiBr_3$ in methanol and heating to 80°C while stirring. The end members $Cs_3Bi_2Br_9$ and $Cs_3Bi_2I_9$ were prepared directly from HBr or HI respectively. Once the precursors had fully dissolved, the solutions were allowed to cool naturally to room temperature, yielding precipitates ranging from vibrant yellow in color for the pure bromide to orange for the mixed anionic phases to a dark red for the fully substituted iodide. These powders were collected *via* vacuum filtration and washed with cold methanol or ether and dried on the benchtop. While attempts were made to prepare thin films of the mixed anionic phases through spin casting, the best conditions for producing single phase films could not be identified and typically resulted in a mixture of the end members.

Laboratory X-ray diffraction was collected on a Bruker D8 diffractometer equipped with a Cu-K_α source (λ_1=1.5406 λ_2=1.5444 Å,). Higher resolution synchrotron X-ray diffraction was performed on the 11-BM beamline at the Advanced Photon Source at Argonne National Lab. Discrete detectors covering an angular range from -6 to 16° 2θ were scanned over a 34° 2θ range, with data points collected every 0.001° 2θ and a scan speed of 0.01°s^1. The resulting patterns were refined using the method Rietveld[1] as implemented within the FullProf suite of software.[2] The optical properties of the polycrystalline powders were characterized using a Perkin-Elmer UV-Vis-NIR Lamda 950 in a diffuse reflectance geometry after mixing into a $BaSO_4$ matrix at a 3 wt% concentration.

Computational

Density Functional Theory (DFT) calculations were performed within periodic boundary conditions using the Vienna Abinitio Simulation Package (VASP) to simulate the effect of iodine substitution on the electronic structure within the $Cs_3Bi_2Br_9$ structure.[3–6] The projector-augmented wave method is used to describe the interaction between valence and core electrons in all calculations, and scalar-relativistic pseudopotentials were used, with Bi 5d electrons explicitly treated as valence.[7] All possible symmetry-inequivalent iodine-substituted structures within the unit cell of $Cs_3Bi_2Br_9$ were exhaustively generated through the SOD program.[8] Geometry relaxation and energetic ordering of these structures was then performed using the PBEsol functional,[9] which has been used to successfully describe the structural properties of $Cs_3Bi_2Br_9$ and other bismuth halides in previous reports.[10–12] Each structure was optimized until the force on each atom did not exceed $0.01\,\mathrm{eV\,Å^{-1}}$, and the lowest energy polymorph for each substitutional configuration was then used as the basis for electronic structure calculations. The electronic properties, density of states and band structures were calculated using the HSE06 functional,[13] which with the addition of spin-orbit coupling, has previously been used to accurately predict the electronic structures, including band gaps, of bismuth halide semiconductors.[11,14,15] A cutoff energy of 400 eV and a k-mesh of $3\times3\times3$ was used in all calculations.

The equilibrium substituted structures reported are provided in an online repository: https://github.com/SMTG-UCL/cesium-bismuth-halides.

References

(1) Rietveld, H. M. A profile refinement method for nuclear and magnetic structures. *Journal of Applied Crystallography* **1969**, *2*, 65.

(2) Rodríguez-Carvajal, J. Recent advances in magnetic structure determination by neutron powder diffraction. *Physica B* **1993**, *192*, 55–69.

(3) Kresse, G.; Hafner, J. *Ab initio* molecular dynamics for liquid metals. *Physical Review B* **1993**, *47*, 558–561.

(4) Kresse, G.; Hafner, J. Ab initio molecular-dynamics simulation of the liquid-metal amorphous-semiconductor transition in germanium. *Physical Review B* **1994**, *49*, 14251–14269.

(5) Kresse, G.; Furthmüller, J. Efficiency of ab initio total energy calculations for metals and semiconductors using a plane wave basis set. *Computational Materials Science* **1996**, *6*, 15.

(6) Kresse, G.; Furthmüller, J. Efficiency of ab initio total energy calculations for metals and semiconductors using a plane wave basis set. *Computational Materials Science* **1996**, *6*, 15–50.

(7) Blöchl, P. E.; Jepsen, O.; Andersen, O. K. Improved tetrahedron method for Brillouin-zone integrations. *Phys. Rev.B* **1994**, *49*, 16223.

(8) Grau-Crespo, R.; Hamad, S.; Catlow, C. R. A.; de Leeuw, N. H. Symmetry-adapted configurational modelling of fractional site occupancy in solids. *Journal of Physics: Condensed Matter* **2007**, *19*, 256201.

(9) Perdew, J. P.; Ruzsinszky, A.; Csonka, G. I.; Vydrov, O. a.; Scuseria, G. E.; Constantin, L. A.; Zhou, X.; Burke, K. Restoring the Density-Gradient Expansion for Exchange in Solids and Surfaces. *Physical Review Letters* **2008**, *100*, 136406.

(10) Savory, C. N.; Walsh, A.; Scanlon, D. O. Can Pb-Free Halide Double Perovskites Support High-Efficiency Solar Cells? *ACS Energy Letters* **2016**, *1*, 949–955.

(11) Bass, K. K.; Estergreen, L.; Savory, C. N.; Buckeridge, J.; Scanlon, D. O.; Djurovich, P. I.; Bradforth, S. E.; Thompson, M. E.; Melot, B. C. Vibronic Structure in Room Temperature Photoluminescence of the Halide Perovskite $Cs_3Bi_2Br_9$. *Inorganic Chemistry* **2017**, *56*, 42–45.

(12) Ganose, A. M.; Matsumoto, S.; Buckeridge, J.; Scanlon, D. O. Defect Engineering of Earth-Abundant Solar Absorbers BiSI and BiSeI. *Chemistry of Materials* **2018**, *30*, 3827–3835.

(13) Krukau, A. V.; Vydrov, O. A.; Izmaylov, A. F.; Scuseria, G. E. Influence of the exchange screening parameter on the performance of screened hybrid functionals. *The Journal of Chemical Physics* **2006**, *125*, 224106.

(14) Lehner, A. J.; Fabini, D. H.; Evans, H. A.; Hbert, C.-A.; Smock, S. R.; Hu, J.; Wang, H.; Zwanziger, J. W.; Chabinyc, M. L.; Seshadri, R. Crystal and Electronic Structures of Complex Bismuth Iodides $A_3Bi_2I_9$ (A = K, Rb, Cs) Related to Perovskite: Aiding the Rational Design of Photovoltaics. *Chemistry of Materials* **2015**, *27*, 7137–7148.

(15) Lehner, A. J.; Wang, H.; Fabini, D. H.; Liman, C. D.; Hbert, C.-A.; Perry, E. E.; Wang, M.; Bazan, G. C.; Chabinyc, M. L.; Seshadri, R. Electronic structure and photovoltaic application of BiI_3. *Applied Physics Letters* **2015**, *107*.

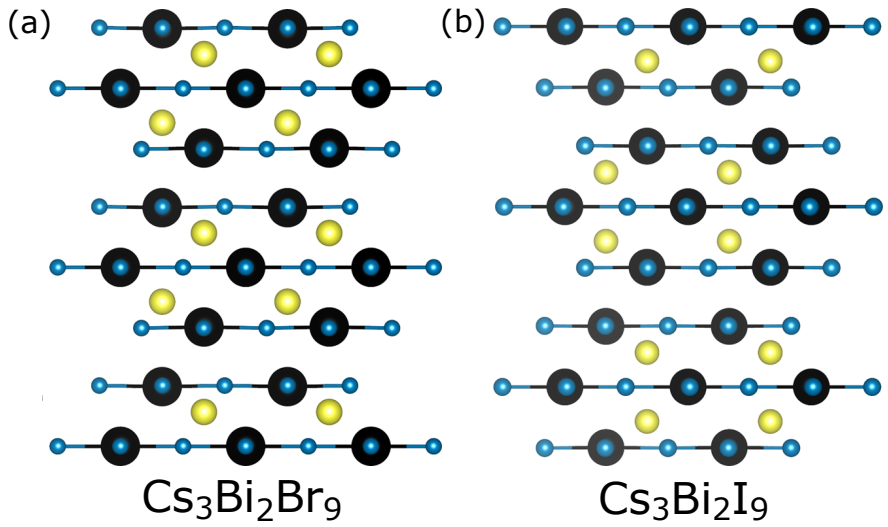

Figure S 1: Comparison of the close-packing sequence in the (a) trigonal bromide and (b) hexagonal iodide structures. Note the bromide results in layers of corner-sharing octahedra whereas the iodide produces dimerized units of face-sharing octahedra as described in the main text.

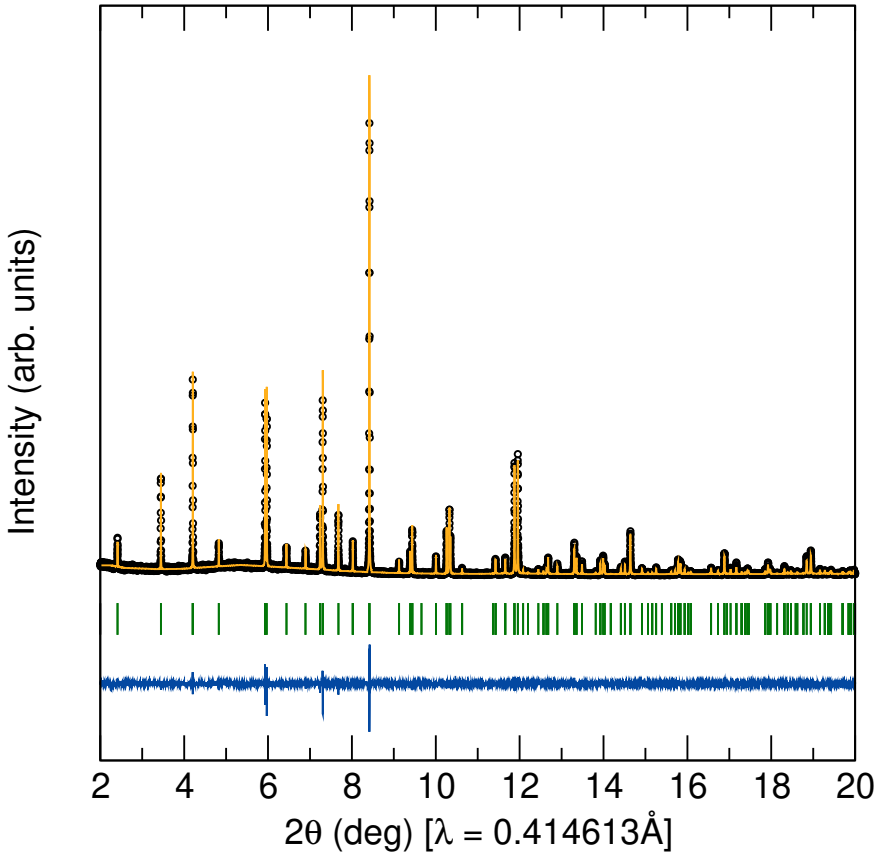

Figure S 2: Results of the Rietveld refinement of the structure for $Cs_3Bi_2Br_9$ against synchrotron X-ray diffraction data collected on the 11-BM beamline (λ=0.414613Å). Details of the fitted parameters can be found in the following table.

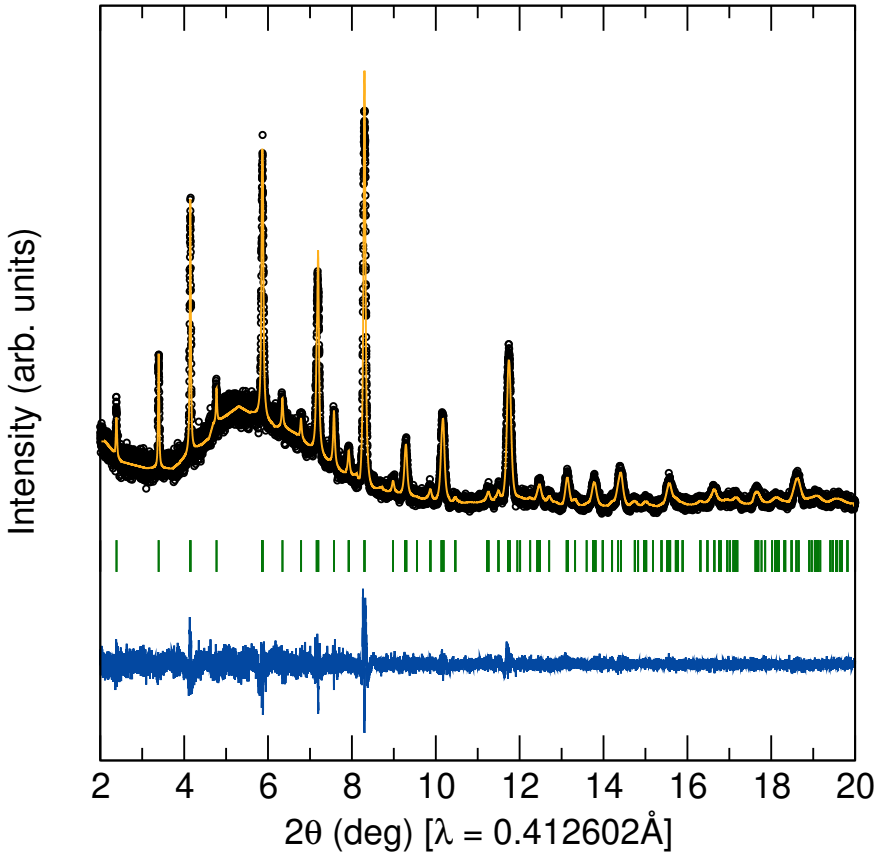

Figure S 3: Results of the Rietveld refinement of the structure for $Cs_3Bi_2Br_8I_1$ against synchrotron X-ray diffraction data collected on the 11-BM beamline (λ=0.412602Å). Details of the fitted parameters can be found in the following table.

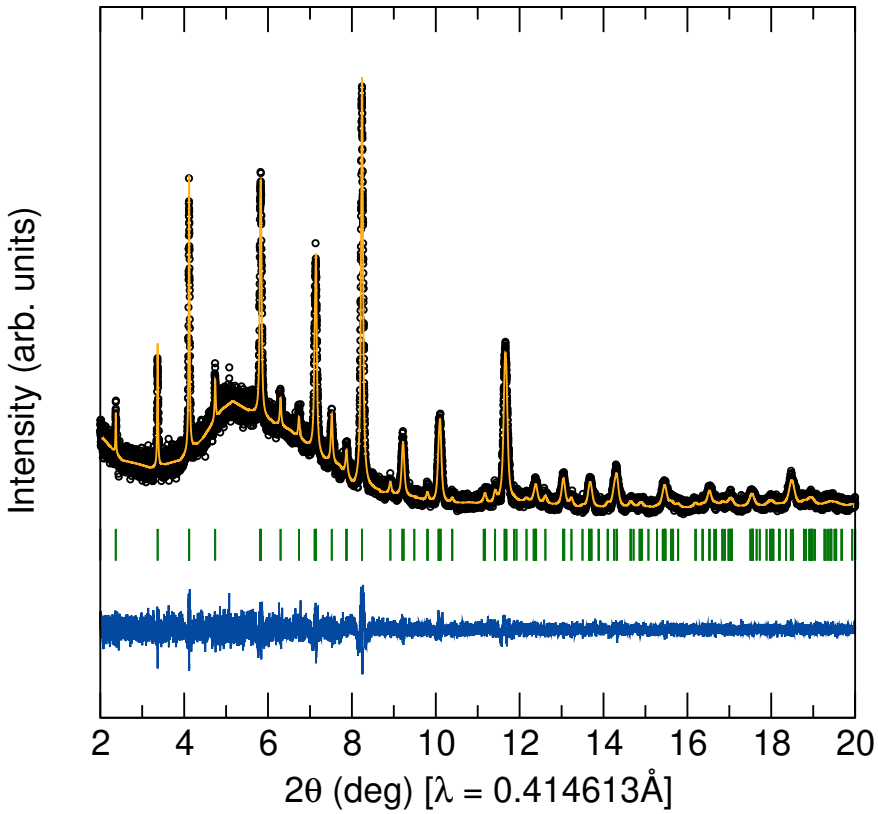

Figure S 4: Results of the Rietveld refinement of the structure for $Cs_3Bi_2Br_7I_2$ against synchrotron X-ray diffraction data collected on the 11-BM beamline (λ=0.412602Å). Details of the fitted parameters can be found in the following table.

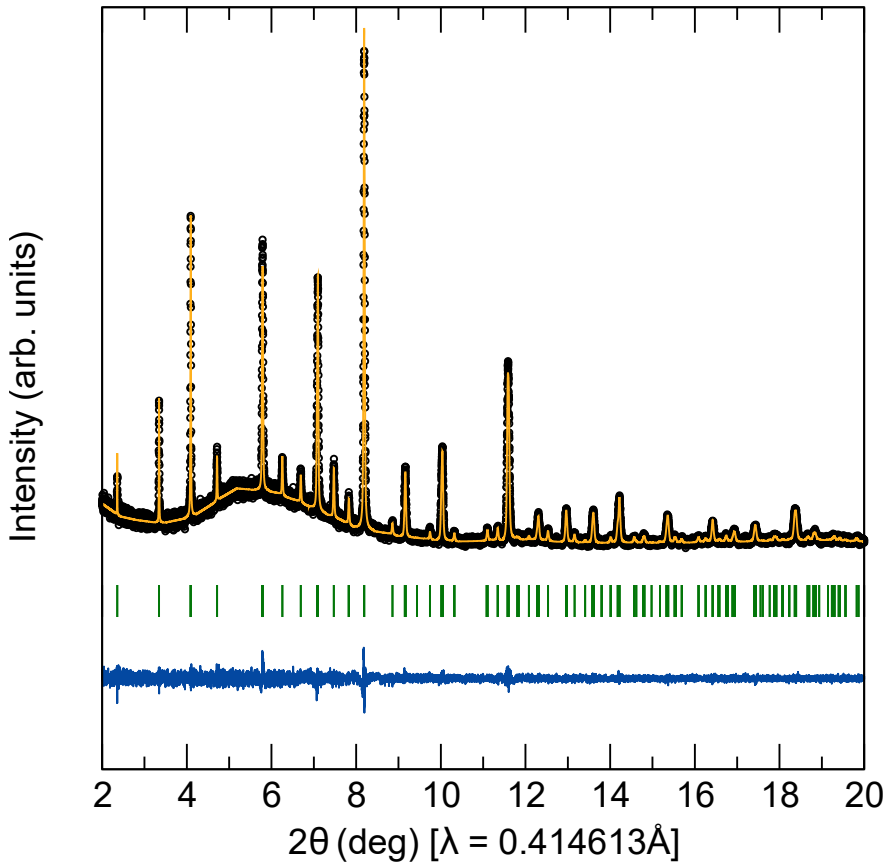

Figure S 5: Results of the Rietveld refinement of the structure for $Cs_3Bi_2Br_6I_3$ against synchrotron X-ray diffraction data collected on the 11-BM beamline (λ=0.414613Å). Details of the fitted parameters can be found in the following table.

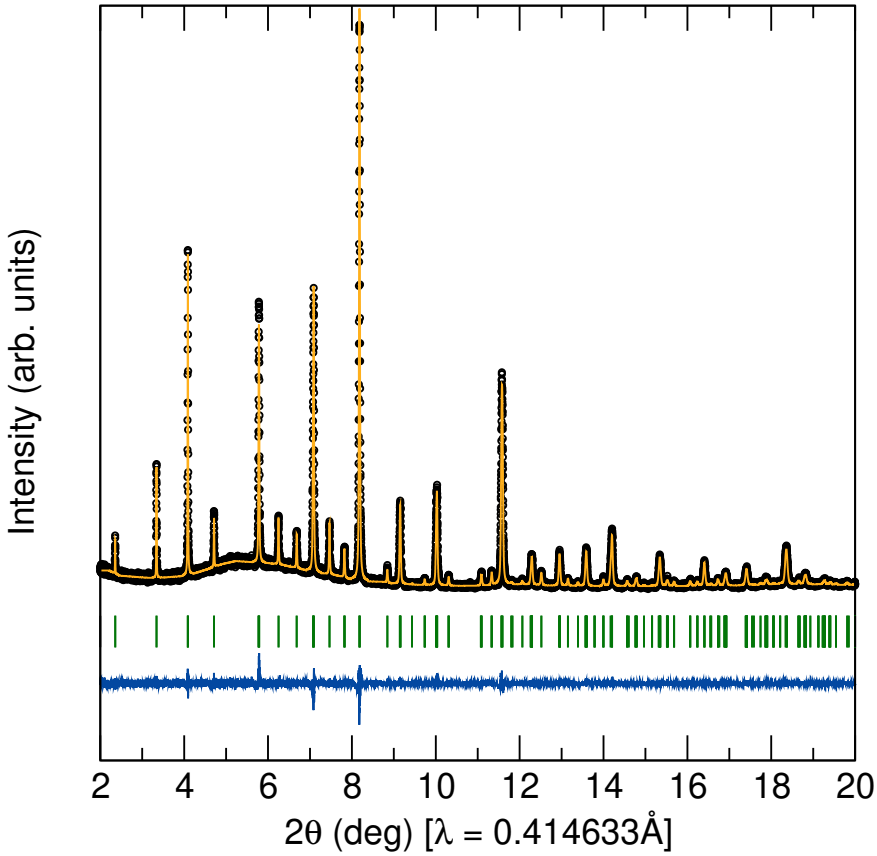

Figure S 6: Results of the Rietveld refinement of the structure for $Cs_3Bi_2Br_5I_4$ against synchrotron X-ray diffraction data collected on the 11-BM beamline (λ=0.414633Å). Details of the fitted parameters can be found in the following table.

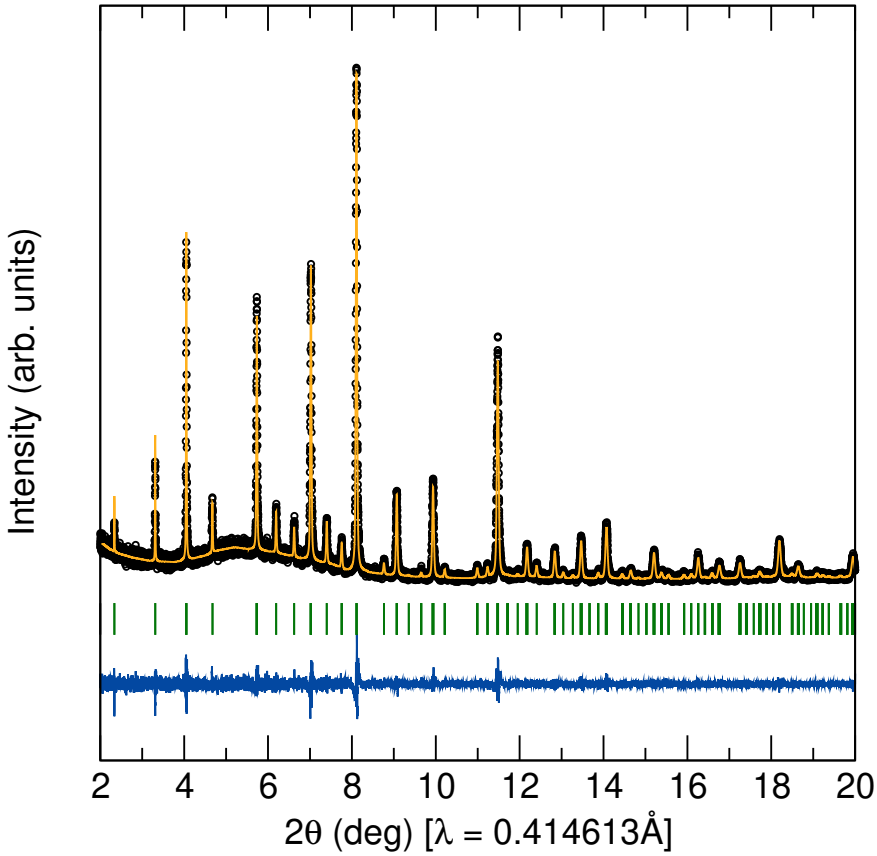

Figure S 7: Results of the Rietveld refinement of the structure for $Cs_3Bi_2Br_4I_5$ against synchrotron X-ray diffraction data collected on the 11-BM beamline (λ=0.414613Å). Details of the fitted parameters can be found in the following table.

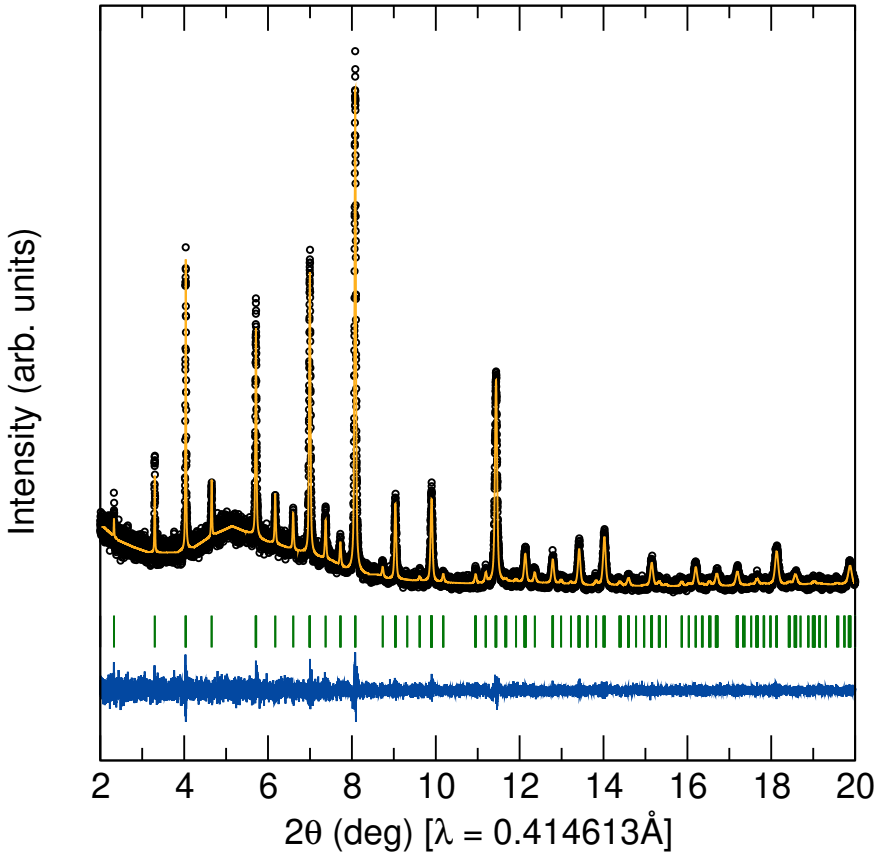

Figure S 8: Results of the Rietveld refinement of the structure for $Cs_3Bi_2Br_3I_6$ against synchrotron X-ray diffraction data collected on the 11-BM beamline (λ=0.414613Å). Details of the fitted parameters can be found in the following table.

Table S 1: Results of the Rietveld refinement of the structure for $Cs_3Bi_2Br_9$ against synchrotron X-ray diffraction data collected on the 11-BM beamline (λ=0.414613Å). a = 7.96150(2), c = 9.84784(3). R_{Bragg} =3.42%

atom	x	y	z	Occupancy
Bi1	0.6667	0.3333	0.1919	0.3333
Cs1	0.0000	0.0000	0.0000	0.1667
Cs2	0.6667	0.3333	0.6662	0.3333
Br1	0.5000	0.5000	0.0000	0.5000
Br2	0.3353	0.1676	0.3399	1.0000

atom	β_{11}	β_{22}	β_{33}	β_{12}	β_{13}	β_{23}
Bi1	0.0080	0.0080	0.0027	0.0040	0.0000	0.0000
Cs1	0.0224	0.0224	0.0176	0.0112	0.0000	0.0000
Cs2	0.0217	0.0217	0.0097	0.0108	0.0000	0.0000
Br1	0.0347	0.0347	0.0127	0.0263	-0.0060	0.0060
Br2	0.0126	0.0230	0.0114	0.0063	0.0018	0.0009

Table S 2: Results of the Rietveld refinement of the structure for $Cs_3Bi_2Br_8I$ against synchrotron X-ray diffraction data collected on the 11-BM beamline (λ=0.412602Å). a = 8.0467(2), c = 9.9169(3). R_{Bragg} =4.21%

atom	x	y	z	Occupancy
Bi1	0.6667	0.3333	0.1880	0.3333
Cs1	0.0000	0.0000	0.0000	0.1667
Cs2	0.6667	0.3333	0.6722	0.3333
Br1	0.5000	0.5000	0.0000	0.4921
I1	0.5000	0.5000	0.0000	0.0079
Br2	0.3347	0.1673	0.3378	0.7936
I2	0.3347	0.1673	0.3378	0.2064

atom	β_{11}	β_{22}	β_{33}	β_{12}	β_{13}	β_{23}
Bi1	0.0134	0.0134	0.0033	0.0067	0.0000	0.0000
Cs1	0.0298	0.0298	0.0100	0.0149	0.0000	0.0000
Cs2	0.0305	0.0305	0.0132	0.0152	0.0000	0.0000
Br1	0.0395	0.0395	0.0121	0.0297	-0.0090	0.0090
I1	0.0395	0.0395	0.0121	0.0297	-0.0090	0.0090
Br2	0.0294	0.0330	0.0087	0.0147	-0.0008	-0.0004
I2	0.0294	0.0330	0.0087	0.0147	-0.0008	-0.0004

Table S 3: Results of the Rietveld refinement of the structure for $Cs_3Bi_2Br_7I_2$ against synchrotron X-ray diffraction data collected on the 11-BM beamline (λ=0.412602Å). a = 8.1073(2), c = 9.9778(3). R_{Bragg} =2.80%

atom	x	y	z	Occupancy
Bi1	0.6667	0.3333	0.1869	0.3333
Cs1	0.0000	0.0000	0.0000	0.1667
Cs2	0.6667	0.3333	0.6746	0.3333
Br1	0.5000	0.5000	0.0000	0.4699
I1	0.5000	0.5000	0.0000	0.0301
Br2	0.3306	0.1653	0.3390	0.6158
I2	0.3306	0.1653	0.3390	0.3842

atom	β_{11}	β_{22}	β_{33}	β_{12}	β_{13}	β_{23}
Bi1	0.0097	0.0097	0.0012	0.0048	0.0000	0.0000
Cs1	0.0366	0.0366	0.0052	0.0183	0.0000	0.0000
Cs2	0.0244	0.0244	0.0109	0.0122	0.0000	0.0000
Br1	0.0469	0.0469	0.0176	0.0383	0.0003	-0.0003
I1	0.0469	0.0469	0.0176	0.0383	0.0003	-0.0003
Br2	0.0244	0.0347	0.0027	0.0122	0.0120	0.0060
I2	0.0244	0.0347	0.0027	0.0122	0.0120	0.0060

Table S 4: Results of the Rietveld refinement of the structure for $Cs_3Bi_2Br_6I_3$ against synchrotron X-ray diffraction data collected on the 11-BM beamline (λ=0.414613Å). a = 8.1626(1), c = 10.0316(1). R_{Bragg} =3.73%

atom	x	y	z	Occupancy
Bi1	0.6667	0.3333	0.1843	0.3333
Cs1	0.0000	0.0000	0.0000	0.1667
Cs2	0.6667	0.3333	0.6761	0.3333
Br1	0.5000	0.5000	0.0000	0.4412
I1	0.5000	0.5000	0.0000	0.0588
Br2	0.3313	0.1656	0.3383	0.4509
I2	0.3313	0.1656	0.3383	0.5491

atom	β_{11}	β_{22}	β_{33}	β_{12}	β_{13}	β_{23}
Bi1	0.0096	0.0096	0.0027	0.0048	0.0000	0.0000
Cs1	0.0261	0.0261	0.0121	0.0131	0.0000	0.0000
Cs2	0.0253	0.0253	0.0109	0.0127	0.0000	0.0000
Br1	0.0423	0.0423	0.0174	0.0301	-0.0042	0.0042
I1	0.0423	0.0423	0.0174	0.0301	-0.0042	0.0042
Br2	0.0238	0.0279	0.0109	0.0119	0.0098	0.0049
I2	0.0238	0.0279	0.0109	0.0119	0.0098	0.0049

Table S 5: Results of the Rietveld refinement of the structure for $Cs_3Bi_2Br_5I_4$ against synchrotron X-ray diffraction data collected on the 11-BM beamline (λ=0.414633Å). a = 8.21314(6), c = 10.08512(9). R_{Bragg} =3.38%

atom	x	y	z	Occupancy
Bi1	0.6667	0.3333	0.1827	0.3333
Cs1	0.0000	0.0000	0.0000	0.1667
Cs2	0.6667	0.3333	0.6776	0.3333
Br1	0.5000	0.5000	0.0000	0.3812
I1	0.5000	0.5000	0.0000	0.1188
Br2	0.3303	0.1651	0.3378	0.2852
I2	0.3303	0.1651	0.3378	0.7148

atom	β_{11}	β_{22}	β_{33}	β_{12}	β_{13}	β_{23}
Bi1	0.0083	0.0083	0.0030	0.0041	0.0000	0.0000
Cs1	0.0289	0.0289	0.0160	0.0144	0.0000	0.0000
Cs2	0.0227	0.0227	0.0128	0.0113	0.0000	0.0000
Br1	0.0482	0.0482	0.0208	0.0322	-0.0070	0.0070
I1	0.0482	0.0482	0.0208	0.0322	-0.0070	0.0070
Br2	0.0187	0.0259	0.0110	0.0094	0.0045	0.0023
I2	0.0187	0.0259	0.0110	0.0094	0.0045	0.0023

Table S 6: Results of the Rietveld refinement of the structure for $Cs_3Bi_2Br_4I_5$ against synchrotron X-ray diffraction data collected on the 11-BM beamline (λ=0.414613Å). a = 8.2881(1), c = 10.1679(2). R_{Bragg} =3.71%

atom	x	y	z	Occupancy
Bi1	0.6667	0.3333	0.1816	0.3333
Cs1	0.0000	0.0000	0.0000	0.1667
Cs2	0.6667	0.3333	0.6799	0.3333
Br1	0.5000	0.5000	0.0000	0.3895
I1	0.5000	0.5000	0.0000	0.1105
Br2	0.3292	0.1646	0.3365	0.1098
I2	0.3292	0.1646	0.3365	0.8902

atom	β_{11}	β_{22}	β_{33}	β_{12}	β_{13}	β_{23}
Bi1	0.0093	0.0093	0.0036	0.0046	0.0000	0.0000
Cs1	0.0281	0.0281	0.0155	0.0140	0.0000	0.0000
Cs2	0.0212	0.0212	0.0152	0.0106	0.0000	0.0000
Br1	0.0370	0.0370	0.0211	0.0174	-0.0113	0.0113
I1	0.0370	0.0370	0.0211	0.0174	-0.0113	0.0113
Br2	0.0274	0.0222	0.0131	0.0137	0.0086	0.0043
I2	0.0274	0.0222	0.0131	0.0137	0.0086	0.0043

Table S 7: Results of the Rietveld refinement of the structure for $Cs_3Bi_2Br_3I_6$ against synchrotron X-ray diffraction data collected on the 11-BM beamline (λ=0.414613Å). a = 8.3173(2), c = 10.2087(3). R_{Bragg} =4.38%

atom	x	y	z	Occupancy
Bi1	0.6667	0.3333	0.1824	0.3333
Cs1	0.0000	0.0000	0.0000	0.1667
Cs2	0.6667	0.3333	0.6800	0.3333
Br1	0.5000	0.5000	0.0000	0.2955
I1	0.5000	0.5000	0.0000	0.2045
Br2	0.3299	0.1649	0.3386	0.0757
I2	0.3299	0.1649	0.3386	0.9243

atom	β_{11}	β_{22}	β_{33}	β_{12}	β_{13}	β_{23}
Bi1	0.0076	0.0076	0.0051	0.0038	0.0000	0.0000
Cs1	0.0197	0.0197	0.0297	0.0098	0.0000	0.0000
Cs2	0.0174	0.0174	0.0183	0.0087	0.0000	0.0000
Br1	0.0419	0.0419	0.0332	0.0138	-0.0162	0.0162
I1	0.0419	0.0419	0.0332	0.0138	-0.0162	0.0162
Br2	0.0280	0.0205	0.0105	0.0140	0.0087	0.0044
I2	0.0280	0.0205	0.0105	0.0140	0.0087	0.0044